

Crystal Growth, Structure, and Spectral Properties of $\text{Cr}^{4+}:\text{Ca}_2(\text{Al}_{1.8}\text{Ga}_{0.2})\text{SiO}_7$ ^①

WANG Dong-Mei^{a, b} LIU Guo-Jiao^{b, c} LIU Le-Hui^{b, c}
YUAN Fei-Fei^{b, c} ZHANG Li-Zhen^{b, d②} LIN Zhou-Bin^{b, c②}

^a (College of Chemistry and Materials Science, Fujian Normal University, Fuzhou 350007, China)

^b (Key Laboratory of Optoelectronic Materials Chemistry and Physics, Fujian Institute of Research on the Structure of Matter, Chinese Academy of Sciences, Fuzhou 350002, China)

^c (Fujian Science & Technology Innovation Laboratory for

Optoelectronic Information of China, Fuzhou 350108, China)

^d (State Key Laboratory of Structural Chemistry, Fuzhou 350002, China)

ABSTRACT A new crystal, $\text{Ca}_2(\text{Al}_{1.8}\text{Ga}_{0.2})\text{SiO}_7$, was obtained by substituting Ga^{3+} ions for some Al^{3+} ions in $\text{Ca}_2\text{Al}_2\text{SiO}_7$ crystal. The growth, structure and optical spectroscopic properties of Cr^{4+} -doped $\text{Ca}_2(\text{Al}_{1.8}\text{Ga}_{0.2})\text{SiO}_7$ were studied. It shows strong absorption at 693 and 762 nm and a broad emission band with peak wavelength at 1223 nm. Both the absorption and emission peaks of Cr^{4+} -doped $\text{Ca}_2(\text{Al}_{1.8}\text{Ga}_{0.2})\text{SiO}_7$ crystal are red-shifted in comparison with that of Cr^{4+} -doped $\text{Ca}_2\text{Al}_2\text{SiO}_7$ crystal due to its weaker lattice field. The investigation results show that there is only one kind of tetrahedral site for Cr^{4+} occupation in the lattice of $\text{Ca}_2(\text{Al}_{1.8}\text{Ga}_{0.2})\text{SiO}_7$ crystal.

Keywords: crystal structure, optical properties, crystalline field, single crystal growth;

DOI: 10.14102/j.cnki.0254-5861.2011-3066

1 INTRODUCTION

Tunable solid-state laser, whose output laser wavelength is continuously adjustable in a certain range, has been widely used in the medicine field, ultra-short pulse generation, and communication^[1, 2]. It is widely thought that the Cr^{4+} ion is a desired broadband near infrared luminescent center in the weak crystal field materials^[3], since its broad emission band ranging from 1.13 to 1.63 μm meets the optical telecommunication windows^[4]. Besides broadband emission, it also has a wide absorption band, which is beneficial to the absorption of pump energy. In addition, the four-level energy band structure benefits the near infrared laser output with continuous pump or pulse laser pump^[4]. These interesting characteristics make Cr^{4+} -doped crystals apply in novel broad-band amplifier^[5, 6], optical communications, eye-safe imaging, and spectroscopy^[4]. Benefiting from its interesting characteristic in tunable laser applications, Cr^{4+} ion doped crystals have received increasing attention^[6-9] and a number

of Cr^{4+} ion doped crystals have been grown and studied, such as Mg_2SiO_4 ^[10], YAG ^[11], Y_2SiO_5 ^[12], $\text{Li}_2\text{MgSiO}_4$ ^[13], SrAl_2O_4 ^[12], $\text{CaGd}_4(\text{SiO}_4)_3\text{O}$ ^[14] and so on. Among them, $\text{Cr}^{4+}:\text{Mg}_2\text{SiO}_4$ and $\text{Cr}^{4+}:\text{YAG}$ crystals have been commercialized. Nonetheless, these materials have several drawbacks. One is the serious nonradiative transition which results in the low laser output efficiency. Another problem is the undesired presence of Cr^{3+} along with Cr^{4+} , leading to rather complicated optical spectra and low laser output efficiency^[8]. Therefore, it is necessary to explore new tunable laser materials which exhibit only Cr^{4+} ions and a weaker crystal field.

In the melilite crystals of $\text{Ca}_2\text{Al}_2\text{SiO}_7$ (CAS) and $\text{Ca}_2\text{Ga}_2\text{SiO}_7$ (CGS), only the tetrahedral site is available, which makes the substitution of Cr^{4+} easy to happen^[15, 16]. Sugimoto A. et al.^[15] have reported the spectroscopic properties of Cr-doped melilite crystals. Larry D. Merkle et al.^[16] have studied the crystal growth and spectroscopic properties of $\text{Cr}^{4+}:\text{CAS}$ and $\text{Cr}^{4+}:\text{CGS}$. The corresponding

Received 10 December 2020; accepted 22 January 2021

① This work was supported by the National Natural Science Foundation of China (No. 61775217)

② Corresponding authors. E-mails: lzzhang@fjirsm.ac.cn and lzb@fjirsm.ac.cn

peaks in absorption and emission spectra of CAS and CGS have been ascribed to Cr^{4+} in the tetrahedral sites and a weak crystal field^[17]. Since CAS and CGS are analogous to the melilite group of minerals^[15], it may not fundamentally change the structure by substituting Ga^{3+} ions for some Al^{3+} ions in CAS crystal. But the distortion of tetrahedron may be increased by doping Ga^{3+} ions in $\text{Ca}_2\text{Al}_2\text{SiO}_7$ to increase the ionic size in this site, so that the average cation-ligand distance at tetrahedron site may be large, which might lead to a weaker crystal field^[18]. With this in mind, a new tunable laser crystal was obtained, in which tetrahedron is the only site, and Cr^{4+} ions in that site should encounter a weaker crystal field.

In this paper, a large single crystal of $\text{Cr}^{4+}:\text{Ca}_2(\text{Al}_{1.8}\text{Ga}_{0.2})\text{SiO}_7$ with dimensions of $\Phi 20 \times 30 \text{ mm}^3$ was grown successfully by the Cz technology. The crystallographic structure of $\text{Cr}^{4+}:\text{Ca}_2(\text{Al}_{1.8}\text{Ga}_{0.2})\text{SiO}_7$ was researched. Furthermore, more details of crystal spectra, including absorption and fluorescence spectra and fluorescence decay kinetics, were reported.

2 EXPERIMENTAL

2.1 Synthesis polycrystalline

The chemicals CaCO_3 , Ga_2O_3 , SiO_2 , Cr_2O_3 and Al_2O_3 (purity 99.99%) used as raw materials were calculated in the stoichiometric amounts of $x\text{Cr}^{4+}:\text{Ca}_2(\text{AlGa})\text{SiO}_7$ ($x = 0, 1, 2, 3$ at.%) ($\text{Al}_2\text{O}_3:\text{Ga}_2\text{O}_3 = 1:1$). The powder of $x\text{Cr}^{4+}:\text{Ca}_2(\text{AlGa})\text{SiO}_7$ ($x = 0, 1, 2, 3$ at.%) was synthesized by conventional solid-state reaction. The mixture was evenly ground in an agate mortar, and pressed to pellets which were placed into an alumina crucible and calcined at 980°C for 5 hours in the furnace in order to eliminate the absorbed water in the materials and decompose the carbonate. Then put them into the muffle furnace and heat again at 1300°C for 10 hours to perform the solid state reaction. Finally, $\text{Cr}^{4+}:\text{Ca}_2(\text{AlGa})\text{SiO}_7$ powders were obtained.

2.2 Growth crystal

$\text{Ca}_2(\text{AlGa})\text{SiO}_7$ could melt congruently, which makes it possible to be grown by the Cz method. The molar concentration of doped Cr ions was 0.5 at% in the $\text{Cr}^{4+}:\text{Ca}_2(\text{AlGa})\text{SiO}_7$ polycrystalline material which was then loaded into an Ir crucible with the size of $\Phi 45 \times 50 \text{ mm}^3$ and heated by a 2-kHz radio 25 kHz mid-frequency induction furnace (DJL-400) in the N_2 atmosphere. An $[100]$ oriented $\text{Ca}_2(\text{AlGa})\text{SiO}_7$ single crystal was used as the seed. The

crystal was grown at a pulling rate of $0.5 \sim 1 \text{ mm/h}$ and a rotating rate of $5 \sim 15 \text{ rpm}$. At the end of growth process, the crystal was pulled slowly out from the melt, followed by cooling to room temperature at an annealing rate of $15 \sim 20^\circ\text{C/h}$. The concentration of Cr^{4+} ions in $\text{Ca}_2(\text{AlGa})\text{SiO}_7$ crystal was measured by inductively coupled plasma-atomic emission spectrometry (ICP-AES). Meanwhile, the rough contents of Ca, Al, Ga and Si were measured by the energy-dispersive spectrometry (EDS).

2.3 Phase identification

The powder X-ray diffraction (XRD) patterns of the traditional solid state synthesis products and as-grown crystal were measured by Miniflex 600 power diffractometer with $\text{Cu-K}\alpha$ radiation. The data were collected in the angular range of $2\theta = 10 \sim 80^\circ$ with a scan step width of 0.02° and a scan speed of $5^\circ/\text{min}$. The XRD data were also collected in the 2θ range of $10 \sim 80^\circ$ with a step of 0.02° and an exposure of 7 s at every point for further Rietveld refinements. And the HighScore Plus software was used to perform Rietveld refinements. A pseudo-Voigt function was selected to describe the line profiles. The structure parameters and atomic coordinates of $\text{Ca}_2\text{Al}_2\text{SiO}_7$ crystal were used as the starting model for the iteration procedure.

2.4 Structure determination and element analysis

The structure of the grown crystal was determined based on its single-crystal XRD data which were collected by Rigaku ROD, Synergy Custom system, HyPix diffractometer equipped with mirror-monochromatic $\text{GaK}\alpha$ radiation at 100 K. A single crystal with dimensions of $0.3 \text{ mm} \times 0.3 \text{ mm} \times 0.96 \text{ mm}$ was selected and used for data collection. The SHELXT^[19] structure solution program using Intrinsic Phasing and the SHELXL^[20] refinement package using least-squares minimization were used to solve the structure.

2.5 Spectra properties

A polished rectangular wafer ($3.12 \text{ mm} \times 3.23 \text{ mm} \times 0.96 \text{ mm}$) was used for spectral measurements. Since the crystal cleavages seriously, the optical spectra were recorded with the incident light only perpendicular to the optic c -axis ($E \perp c$). The absorption spectra were measured by a Perkin Elmer UV-VIS-NIR spectrometer (Lambda-950) in the range of $250 \sim 1200 \text{ nm}$ at room temperature. The emission spectra with 694 nm excitation and fluorescence lifetime were measured using the Edinburgh Analysis Instruments FSL980 spectrophotometer with Xenon lamp as the light source at 77 K.

2.6 X-ray photoelectron spectroscopy

X-ray photoelectron spectroscopy (XPS) measurement was carried out using AlK α X-ray radiation operated at 150 W (Thermo Scientific Escalab 250Xi, USA). The shift of the bonding energy due to the relative surface charging was corrected using the C 1s level at 284.8 eV as an internal standard.

3 RESULTS AND DISCUSSION

3.1 X-ray powder diffraction

In order to investigate the influence of Cr⁴⁺ substitution on the microstructure and phase composition of Cr⁴⁺:Ca₂(AlGa)SiO₇ compounds, the powder XRD patterns of xCr⁴⁺:Ca₂(AlGa)SiO₇ (x = 0, 1, 2, 3 at.%) were analyzed and

shown in Fig. 1a. As displayed in this figure, all of the diffraction patterns are consistent with the standard XRD patterns of Ca₂Al₂SiO₇ (PDF#79-1726), indicating that the Cr doped in the crystal with different concentrations did not change the structure. The lattice cell parameters of Ca₂Al₂SiO₇ powders with different doping concentrations were calculated and shown in Fig. 1b. It is clear that the lattice cell of xCr⁴⁺:Ca₂(AlGa)SiO₇ shrinks gradually with the elevating of Cr⁴⁺ content. In a tetrahedral coordination system, the ionic radii of Cr⁴⁺, Ga³⁺, Al³⁺ and Si⁴⁺ are 0.41, 0.47, 0.39 and 0.26 Å, respectively^[21, 22]. Once introduced into Ca₂(AlGa)SiO₇, the Cr⁴⁺ ions with smaller ionic radius replace the Ga³⁺ ones, thus causing the shrinkage of lattice cell.

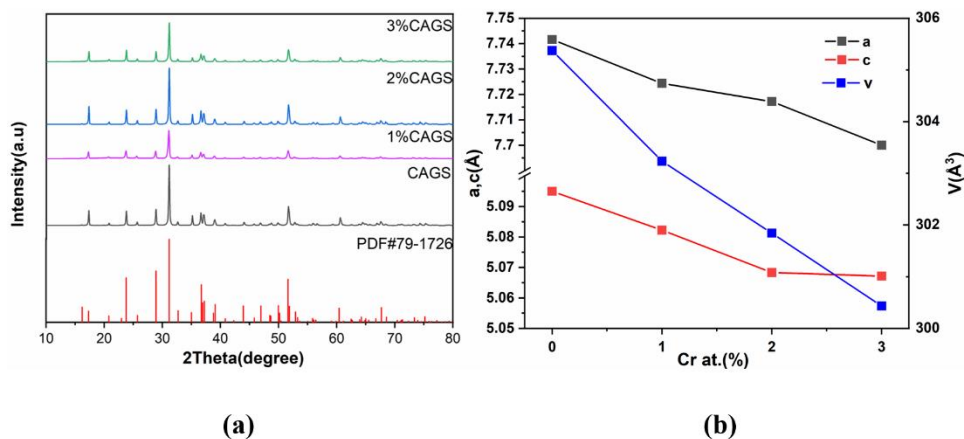


Fig. 1. (a) XRD patterns of powdered xCr⁴⁺:Ca₂(AlGa)SiO₇ (x = 0, 1, 2, 3 at.%) compared with the standard pattern of Ca₂Al₂SiO₇ (PDF#79-1726); (b) Lattice parameters of a, c and v versus the content of Cr⁴⁺ ion

3.2 Growth of the single crystal

The as-grown crystal of Cr⁴⁺:Ca₂(AlGa)SiO₇ with dimensions of $\Phi 20 \times 30 \text{ mm}^3$ was obtained, as shown in Fig. 2a. It can be seen that the grown crystal is deep blue without

obvious impurity. The XRD pattern of the grown Cr⁴⁺:Ca₂(AlGa)SiO₇ crystal is shown in Fig. 2b, which matches the standard XRD pattern (PDF#79-1726) of Ca₂Al₂SiO₇ very well.

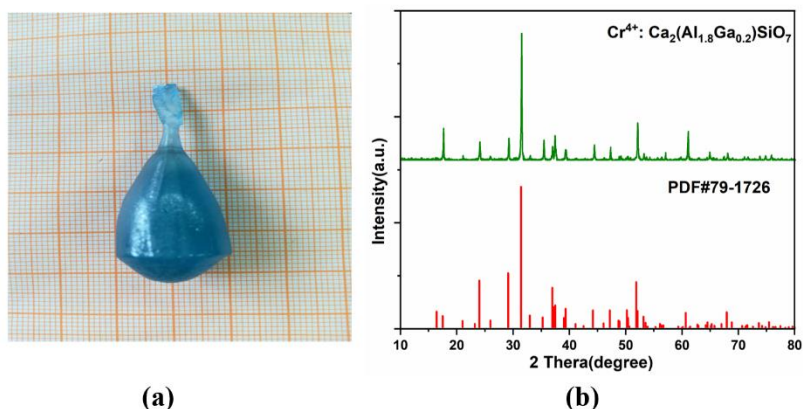


Fig. 2. (a) Cr⁴⁺:Ca₂(Al_{1.8}Ga_{0.2})SiO₇ crystal grown by the Czochralski method; (b) Crystal X-ray diffraction patterns of Cr⁴⁺:Ca₂(Al_{1.8}Ga_{0.2})SiO₇ crystal

In order to confirm the chemical composition of the grown crystal, the contents of Ca:Al:Ga:Si and Cr atoms in the as-grown crystal were measured by ICP-AES and EDS tests. The measured molar ratio of Ca:Al:(Ga + Cr):Si is close to 2:1.8:0.2:1, which means this crystal is inconsistent with the stoichiometric amounts of $\text{Ca}_2(\text{AlGa})\text{SiO}_7$. There are mainly two reasons why the Ga content decreased during the crystal growth procedure. One is that Ga_2O_3 is volatile during the crystal growth, which results in the loss of gallium. The other lies in that the Ga^{3+} ion has bigger radius than Al^{3+} and the segregation coefficient is small. The real chemical formula may be changed into $\text{Cr}^{4+}:\text{Ca}_2(\text{Al}_{1.8}\text{Ga}_{0.2})\text{SiO}_7$, which will be confirmed latter. The concentration of Cr ions in this crystal was measured to be 0.33 at.% (2.2×10^{19} ions/cm³). As the concentration of Cr^{4+} ions in the melt is 0.5 at.%, the segregation coefficient η of Cr^{4+} ion is 0.66.

3.3 Crystal structure

Using Olex2, the structure was solved with the SHELXT^[19] structure solution program using Intrinsic Phasing and refined with the SHELXL^[20] refinement package using least-squares minimization. The structures were also checked for possible missing symmetry with PLATON. The calculated molar ratio of Ca:Al:Ga:Si is 2:1.8:0.2:1, which agrees with the measurement data of ICP and EDS.

The structure of $\text{Ca}_2(\text{Al}_{1.8}\text{Ga}_{0.2})\text{SiO}_7$ is isomorphic to that of $\text{Ca}_2\text{Al}_2\text{SiO}_7$ compound. $\text{Ca}_2(\text{Al}_{1.8}\text{Ga}_{0.2})\text{SiO}_7$ crystallizes into tetragonal crystal system with acentric space group

$P\bar{4}2_1m$ (No. 113)^[23] with $a = b = 7.6964$ Å, $c = 5.0657$ Å, $\beta = 90^\circ$ and $Z = 1$. The asymmetric unit is composed of one unique Ca atom, one unique Si atom, one unique Ga atom, two unique Al atoms, and three unique O atoms. Similar to $\text{Ca}_2\text{Al}_2\text{SiO}_7$, in $\text{Ca}_2(\text{Al}_{1.8}\text{Ga}_{0.2})\text{SiO}_7$, Al(2) and Si co-occupied one crystallographic site with the same occupancy (half for Al(2) and half for Si) and are coordinated with four O atoms to form (Al(2)/Si) O_4 tetrahedron with Al(2)/Si–O bond lengths ranging from 1.652(5) to 1.710(4) Å and O–Al(2)/Si–O bond angles from 101.7(2) to 117.41(18)°. Al(1) co-occupied with Ga at one crystallographic site with different occupancy (0.8 for Al(1) and 0.2 for Ga). The Al(1)/Ga atom is bound to four O atoms to form (Al/Ga) O_4 tetrahedron with the same bond length of 1.767(4) Å and bond angles ranging from 108.41(11)° to 111.6(3)°. Obviously, in the structure, three (Al(2)/Si) O_4 tetrahedra connected with two (Al/Ga) O_4 tetrahedra by sharing the vertex oxygen atoms to create a [(Al/Ga) Si_2O_{15}] structural unit (Fig. 3b). Then the [(Al/Ga) Si_2O_{15}] structural unit links each other with corner-sharing to form [(Al/Ga) Si_2O_7] infinite layers in the *ab* plane (Fig. 3c); these layers were further junctional by CaO_8 polyhedra to build a three-dimensional (3D) framework (Fig. 3c). In this structure the average cation-ligand distance, i.e. Al(1)/Ga–O bond lengths (1.767(4) Å), is larger than that in CAS (1.752 Å) by about 0.86%, so that dopants in that site should encounter a weaker crystal field in these melilites.

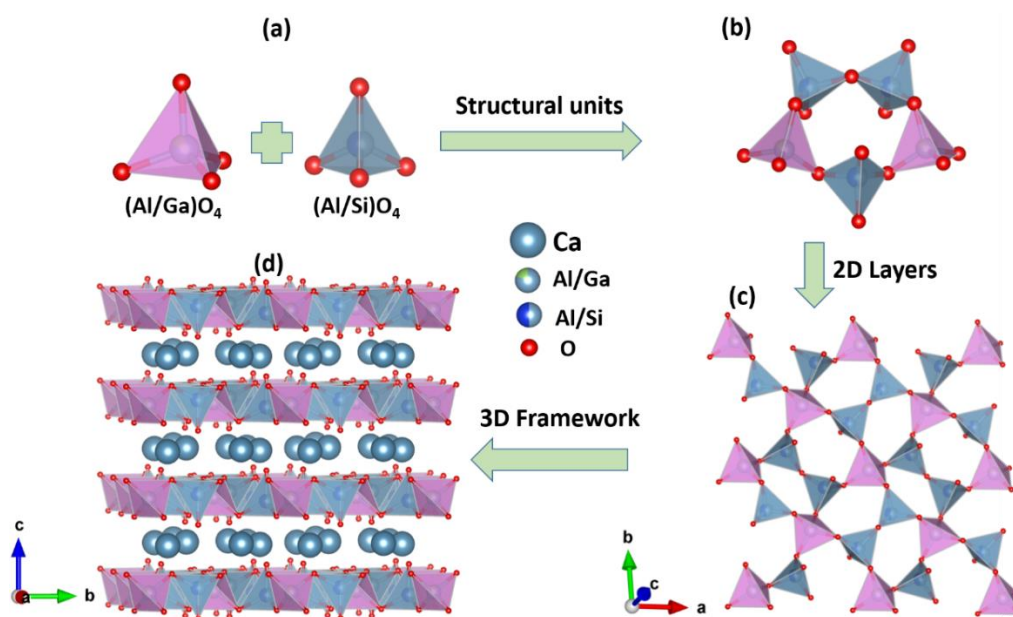


Fig. 3. Ball-and-stick and polyhedral representations for $\text{Ca}_2(\text{Al}_{1.8}\text{Ga}_{0.2})\text{SiO}_7$. (a) The $(\text{Al/Ga})\text{O}_4$ tetrahedron and $(\text{Al/Si})\text{O}_4$ tetrahedron, (b) $[(\text{Al/Ga})_3\text{Si}_2\text{O}_{15}]$ structural unit, (c) 2D $[(\text{Al/Ga})_2\text{SiO}_7]$ layers in the *ab* plane composed of $(\text{Al/Ga})\text{O}_4$ and SiO_4 tetrahedra, and (d) the $[(\text{Al/Ga})_2\text{SiO}_7]$ layers stacked along the *c* axis while Ca^{2+} located at interlayers to balance the charge

3.4 Spectra properties

3.4.1 Absorption spectra

Since the as-grown crystal $\text{Cr}^{4+}:\text{Ca}_2(\text{Al}_{1.8}\text{Ga}_{0.2})\text{SiO}_7$ cleaved seriously, we only measured the absorption spectra recorded at room-temperature with the incident light perpendicular to its optic c -axis (Fig. 4). As can be seen from this figure, the grown crystal shows strong and broad band optical absorption in the visible and near infrared ranges with two peaks at about 693 and 762 nm, corresponding to the transition of Cr^{4+} ions from the ground state $^3\text{A}_2$ to the excited state $^3\text{T}_1$ ^[15]. The absorption cross sections (σ_a) were estimated to be $5.3 \times 10^{-19} \text{ cm}^2$ at 693 nm and $4.7 \times 10^{-19} \text{ cm}^2$ at 762 nm, respectively, which are very suitable for the

commercial AlGaIn LD pumping. Compared with CAS, the absorption peaks have a slight red shift in this crystal.

3.4.2 Emission spectra

As shown in Fig. 4, the emission spectrum of $\text{Cr}^{4+}:\text{Ca}_2(\text{Al}_{1.8}\text{Ga}_{0.2})\text{SiO}_7$ crystal recorded at 77 K is dominated by a broad band emission extending from 1100 to 1500 nm with a full width at half-maximum (FWHM) of 218 nm and the emission peak was at about 1223 nm, ascribed to the $^3\text{T}_2$ to $^3\text{A}_2$ transition of Cr^{4+} ions in a tetrahedral crystal field^[15]. Its peak wavelength is about 30 nm longer than that in the CAS crystal, which means this crystal has weaker crystal field than the CAS one^[16].

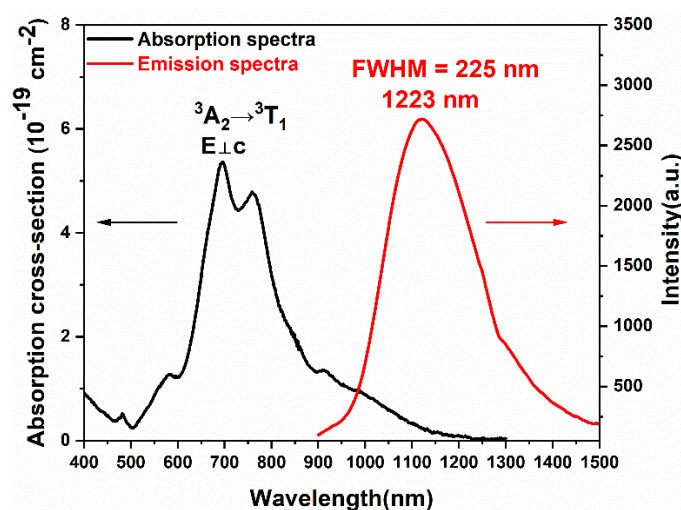


Fig. 4. Absorption spectra (black line) at room temperature and emission spectra (red line) at 77 K with the incident light perpendicular to the optic c -axis of the $\text{Cr}^{4+}:\text{Ca}_2(\text{Al}_{1.8}\text{Ga}_{0.2})\text{SiO}_7$ crystal

Fig. 5 shows the decay curve of $\text{Cr}^{4+}:\text{Ca}_2(\text{Al}_{1.8}\text{Ga}_{0.2})\text{SiO}_7$ crystal with 694 nm excited at 77 K, which exhibits single

exponential character. According to the single-exponential fitting results, the fluorescence lifetime was 22.2 μs .

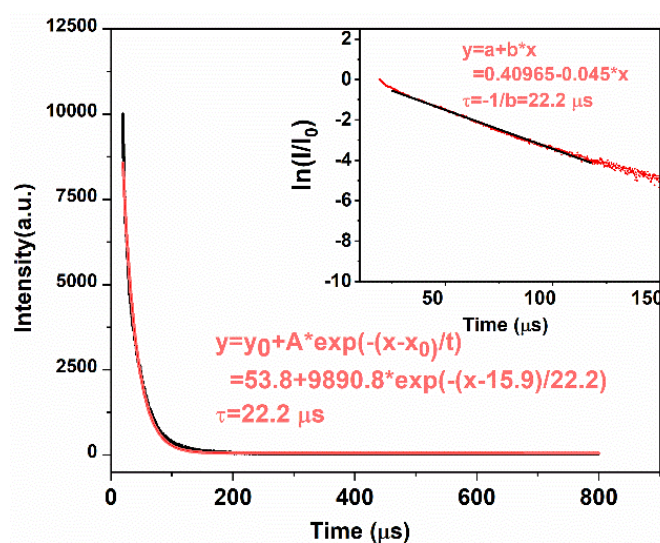


Fig. 5. Fluorescence decay curve of $\text{Cr}^{4+}:\text{Ca}_2(\text{Al}_{1.8}\text{Ga}_{0.2})\text{SiO}_7$ crystal

3.5 X-ray photoelectron spectroscopy analysis

The absorption and emission spectra demonstrate that only Cr^{4+} ion is doped in the $\text{Ca}_2(\text{Al}_{1.8}\text{Ga}_{0.2})\text{SiO}_7$ crystal. Further research is required to confirm only Cr^{4+} ions exist in the as-grown crystal. We investigated the XPS spectra of $\text{Cr}^{4+}:\text{Ca}_2(\text{Al}_{1.8}\text{Ga}_{0.2})\text{SiO}_7$ crystal and Cr_2O_3 . The Cr $2p_{3/2}$ of $\text{Cr}^{4+}:\text{Ca}_2(\text{Al}_{1.8}\text{Ga}_{0.2})\text{SiO}_7$ crystal and Cr_2O_3 XPS spectra are

presented in Fig. 6. As displayed in this figure, the binding energy of Cr $2p_{3/2}$ in Cr_2O_3 is centered at 576.69 eV, which is close to the $\text{Cr}_2\text{O}_3(\text{Cr}^{3+})$ state^[24], and that of the broad Cr $2p_{3/2}$ peak at 576.98 eV corresponds to the Cr^{4+} state^[25]. In general, the corresponding binding energy will increase when the valence state increases. All of those indicate that only the Cr^{4+} ions occur in the $\text{Cr}^{4+}:\text{Ca}_2(\text{Al}_{1.8}\text{Ga}_{0.2})\text{SiO}_7$ crystal.

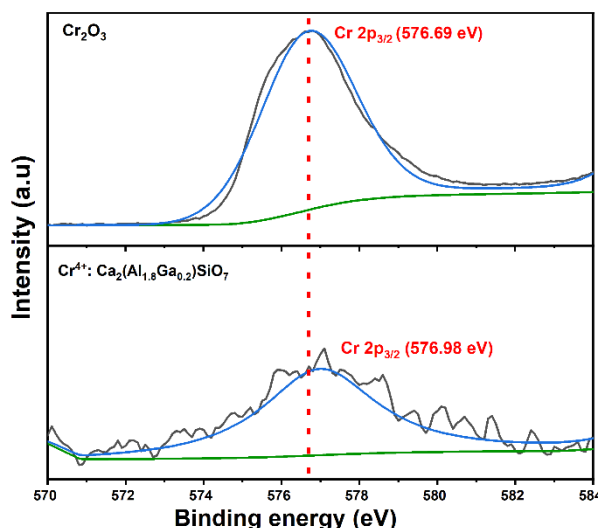


Fig. 6. XPS spectrum of $\text{Cr}^{4+}:\text{Ca}_2(\text{Al}_{1.8}\text{Ga}_{0.2})\text{SiO}_7$ crystal and Cr_2O_3

4 CONCLUSION

In this work, the replacement of Ga^{3+} for part Al^{3+} ions does not fundamentally change the framework of the CAS structure, but the tiny difference of ionic radius and electronegativity between Ga^{3+} and Al^{3+} makes slight alteration on the arrangement and local crystal circumstance of AlO_4 tetrahedra, which results in a longer average cation-ligand distance, so that dopants in that site should encounter a weaker crystal field in its crystal. By this way, a Cr^{4+} -doped $\text{Ca}_2(\text{Al}_{1.8}\text{Ga}_{0.2})\text{SiO}_7$ single crystal with dimensions of $\Phi 20 \times 30 \text{ mm}^3$ was successfully grown by the Cz method, and then the segregation coefficient of Cr^{4+} ions was calculated to be about 0.66. The lattice site with tetrahedral coordination is the only site for Cr^{4+} ions to

occupy in this crystal. The refinement analysis indicated that Cr^{4+} ions most probably replaced the sites of Ga^{3+} ions in GaO_4 tetrahedron. And the Ga_2O_3 is easily volatilize so that the crystal is inconsistent with the stoichiometric amounts and the chemical formula is $\text{Cr}^{4+}:\text{Ca}_2(\text{Al}_{1.8}\text{Ga}_{0.2})\text{SiO}_7$. The absorption cross sections are $5.3 \times 10^{-19} \text{ cm}^2$ and $4.7 \times 10^{-19} \text{ cm}^2$ at 693 and 762 nm, respectively, which is very suitable for the commercial AlGaIn LD pumping. A broad emission band locates at about 1223 nm with a full width at half-maximum of 218 nm and the fluorescence lifetime is about 22.2 μs at 77 K. Compared with CAS crystal, the emission peak wavelength is about 30 nm longer, which means the crystal field in this crystal is weaker than that in CAS. The investigations of spectra and XPS spectrum show that only Cr^{4+} ion is doped in the $\text{Ca}_2(\text{Al}_{1.8}\text{Ga}_{0.2})\text{SiO}_7$ crystal.

REFERENCES

- (1) Cassis, L. A.; Yates, J.; Symons, W. C.; Lodder, R. A. Cardiovascular near-infrared imaging. *J. Near Infrared Spectrosc.* **1998**, 6, A21–A25.
- (2) Samtleben, T. A.; Hulliger, J. LiCaAlF_6 and LiSrAlF_6 : tunable solid state laser host materials. *Opt. Lasers. Eng.* **2005**, 43, 251–262.
- (3) Brik, M. G.; Ogasawara, K. Comparative study of the absorption spectrum of $\text{Li}_2\text{CaSiO}_4:\text{Cr}^{4+}$: first-principles fully relativistic and crystal field calculations. *Opt. Mater.* **2007**, 30, 399–406.
- (4) Sennaroglu, A. Broadly tunable Cr^{4+} -doped solid-state lasers in the near infrared and visible. *Prog. Quantum Electron.* **2002**, 26, 287–352.
- (5) Stoychev, L. I.; Cabrera, H.; Gadedjisso-Tossou, K. S.; Nikolov, I. P.; Sigalotti, P.; Demidovich, A. A.; Suárez-Vargas, J. J.; Mocchiutti, E.; Niemela, J.;

- Baruzzo, M.; Vasiliev, N.; Zaporozhchenko, Y.; Danailov, M. B.; Vacch, A. Pulse amplification in a Cr^{4+} : forsterite single longitudinal mode (SLM) multi-pass amplifier. *Laser Physics*. **2019**, 29, 065801.
- (6) Yamazaki, H.; Tanabe, S. Transparent Cr^{4+} -doped gehlenite ($\text{Ca}_2\text{Al}_2\text{SiO}_7$) glass-ceramics for broadband amplifier. *OSA/OAA* **2003**.
- (7) Okhrimchuk, A. G.; Shestakov, A. V. Performance of $\text{YAG}:\text{Cr}^{4+}$ laser crystal. *Opt. Mater.* **1994**, 3, 1–13.
- (8) Henderson, B.; Gallagher, H. G.; Han, T.; Scott, M. A. Optical spectroscopy and optimal crystal growth of some Cr^{4+} -doped garnets. *J. Phys.: Condens. Matter*. **2000**, 12, 1927–1938.
- (9) Brik, M. G.; Avram, C. N.; Tanaka, I. Crystal field analysis of energy level structure of $\text{LiAlO}_2:\text{Cr}^{4+}$ and $\text{LiGaO}_2:\text{Cr}^{4+}$. *Phys. Stat. Sol.* **2004**, 241, 2501–2507.
- (10) Cormier, G.; Simkin, D. J.; Capobianco, J. A. Fluorescence analysis of chromium-doped forsterite (Mg_2SiO_4). *IEEE J. Quantum Electron.* **1991**, 27, 114–120.
- (11) Mikhailov, V. P.; Zhavoronkov, N. I.; Kuleshov, N. V.; Avtukh, A. S. Saturation of visible absorption in chromium-doped silicates. *Opt. Quantum Electron.* **1995**, 27, 765–767.
- (12) Anino, C.; Thér, J.; Vivien, D. New Cr^{4+} activated compounds in tetrahedral sites for tunable laser applications. *Opt. Mater.* **1997**, 8, 121–128.
- (13) Zhuang, Y.; Zhou, J.; Xie, J.; Teng, Y.; Qiu, J. Temperature-dependent broadband near-infrared luminescence in silicate glass ceramics containing $\text{Li}_2\text{MgSiO}_4:\text{Cr}^{4+}$ nanocrystals. *J. Mater. Res.* **2011**, 25, 1833–1837.
- (14) Denisov, A.; Yumashev, K. V.; Moncorge, R. Saturable absorber $\text{Cr}^{4+}:(\text{Sr,Ca})\text{Gd}_4(\text{SiO}_4)_3\text{O}$ crystals as Q switches for a diode-pumped $\text{Nd}^{3+}:\text{KGd}(\text{WO}_4)_2$ laser. *Appl. Opt.* **2001**, 49, 5413–5416.
- (15) Sugimoto, A.; Nobe, Y.; Yamazaki, T.; Anzai, Y.; Yamagishi, K.; Segawa, Y.; Takei, H. Spectroscopic properties of Cr-doped melilite crystals. *Phys. Chem. Miner.* **1997**, 24, 326–332.
- (16) Merkie, L. D.; Allik, T. H.; Chai, B. H. T. Crystal growth and spectroscopic properties of Cr^{4+} in $\text{Ca}_2\text{Al}_2\text{SiO}_7$ and $\text{Ca}_2\text{Ga}_2\text{SiO}_7$. *Opt. Mater.* **1992**, 1, 91–100.
- (17) Feng, X.; Tanabe, S. Spectroscopy and crystal-field analysis for Cr (IV) in alumino-silicate glasses. *Opt. Mater.* **2002**, 20, 63–72.
- (18) Kück, S. Laser-related spectroscopy of ion-doped crystals for tunable solid-state lasers. *Appl. Phys.* **2014**, 72, 515–562.
- (19) Sheldrick, G. SHELXT: integrating space group determination and structure solution. *Acta Cryst.* **2014**, A70, C1437.
- (20) Sheldrick, G. SHELXT-integrated space-group and crystal-structure determination. *Acta Cryst.* **2015**, 71, 3–8.
- (21) Liu, G.; Liu, L.; Yuan, F.; Huang, Y.; Zhang, L.; Lin, Z. Cr-doped $\text{Ca}_3\text{NbGa}_3\text{Si}_2\text{O}_{14}$: a promising near-infrared tunable laser crystal. *J. Lumin.* **2020**, 228, 117583.
- (22) Shannon, R. D. Revised effective ionic radii and systematic studies of interatomic distances in halides and chalcogenides. *Acta Cryst.* **1976**, A32, 751–767.
- (23) Simondl-Telssre, B.; Vlana, B.; Vlvlen, D.; Lejus, A. M. Optical investigation of $\text{Er}:\text{Ca}_2\text{Al}_2\text{SiO}_7$ and $\text{Yb}:\text{Ca}_2\text{Al}_2\text{SiO}_7$ for laser applications in the near infrared. *Phys. Stat. Sol.* **1996**, 155, 249–262.
- (24) Allen, C.; Tucker, P. M.; Wild, R. K. X-ray photoelectron/augetron spectroscopic study of the initial oxidation of chromium metal. *J. Chem. Soc. Faraday Trans.* **1978**, 74, 1126–1140.
- (25) Chesta, R.; Anek, C.; Mudtorlep, N.; Pennapa, M.; Chanchana, T.; Santi, M. Effect of strong correlation of Mg^{2+} -doped into Cr^{3+} sites of CuCrO_2 on thermoelectric properties. *Integr. Ferroelectr.* **2015**, 165, 45–52.